Cytokeratins of Tumorigenic and Highly Malignant Respiratory Tract Epithelial Cells

Chapter · March 2022

DOI: 10.5772/intechopen.102592

1 author:

Carol A Heckman
Bowling Green State University
93 PUBLICATIONS **1,634** CITATIONS

SEE PROFILE

Chapter

Cytokeratins of Tumorigenic and Highly Malignant Respiratory Tract Epithelial Cells

Carol A. Heckman

Abstract

In malignant airway epithelial cells, structural abnormalities were evident from the cytokeratin organization. To determine whether the cytokeratins themselves were responsible, an *in vitro* model for bronchogenic carcinoma, consisting of three highly malignant lines and three less tumorigenic lines, was studied. Cytokeratins were evaluated by two-dimensional polyacrylamide gel electrophoresis (2D-PAGE). When typical constraints on tumors were relieved by *in vitro* culture, lines showed profiles resembling normal, primary cells. The CK5/CK14 combination, characteristic of basal epithelial layers, was represented by CK6A/CK14. CK17 was invariably present, while CK5, CK7, CK8, CK19, and CK42 content varied. CK19 appeared to substitute for the rarely observed CK18. While lacking the common CK8/CK18 combination of hyperproliferative cells, an invasive, metastasizing line had CK6A/CK7 or CK8 with CK19 suggesting derivation similar to adenocarcinomas. Bands of CK19 and actin migrated to higher pI in tumorigenic and malignant lines than in normal cells. Ubiquitinated acidic cytokeratins with a low isoelectric point (pI) and high molecular weight (MW) showed no consistent differences in lines that differed in growth potential. Type II made up 49–52% of total cytokeratins in nonmalignant lines, whereas highly malignant lines showed lower levels. Posttranslational modifications were identified but could not explain the shortfall of basic cytokeratins.

Keywords: actin, motility, invasion, squamous cell carcinoma, metastasis, cytoskeleton, differentiation

1. Introduction

Intermediate filaments, which are made up of cytokeratins, are responsible for the structural integration and resiliency of the epithelial linings. To build up the 10-nm filament from the molecular level, a subunit is formed by the dimerization of one type I keratin and one type II molecule. These heterodimers attach in an antiparallel arrangement to compose the larger tetrameric subunit common to 10-nm filaments. End-to-end and side-to-side assembly gives rise to the long, flexible filaments seen in images of epithelial cells. When the large number of keratin genes is considered, plus their posttranslational modifications, there is an impressive variety of filament compositions. Each epithelial cell type is characterized by a combination of type I and type II cytokeratins. For example, some of the human cytokeratins discovered recently are highly expressed in the hair follicle [1]. While the cytokeratin profile of a cell depends on selective expression, which in turn

depends on its differentiated state, there is considerable latitude in expression profiles of some cell types.

It has long been suspected that the cytokeratins play a role in growth regulation. Indeed, CK8, CK17, and CK18 have been investigated with respect to their regulatory roles. Several basic or neutral type II proteins, including CK4-CK6, have a conserved site corresponding to Ser/Thr73 of the CK8 sequence. Posttranslational modification (PTM) at CK8 Ser/Thr73 was found downstream of proapoptotic receptor Fas/CD95-mediated c-Jun N-terminal kinase activation (see for review [2]). In different systems, phosphorylation of type II cytokeratins resulted in increased solubility of the filaments and/or collapse of the filament network. These are among the mechanisms contributing to dissolution of intermediate filaments during mitosis, which allows the cell to round up for division [3–5]. Knockout of the most commonly expressed pairs, CK5 and CK14 or CK8 and CK18, is often embryonic or neonatal lethal (see for review, [2]), affirming the importance of these keratins for epithelial cell differentiations in the lining tissues. Cell behavior was directly affected by cytokeratin content, as has been demonstrated by Magin and coworkers. Keratinocytes deficient in all the cytokeratins showed increased softness and invasiveness, which were largely restored by re-expression of CK5/CK14 [6].

The cytokeratins are also subject to complex transcriptional regulation. In the epidermis, the CK6/CK16 pair are induced within a day after injury [7, 8]. The stress-responsive CK6, CK16, and CK17 were all expressed in response to injury in skin and during hyperproliferation in psoriasis, suggesting their upregulation by the transcription factor, Nrf-2 (see for review [9, 10]). CK17 is regulated by several transcription factors as well as by the possible interaction of the ubiquitylated form with STAT3 (see for review [11]). High expression of CK17 in lung adenocarcinoma was predictive of poor overall survival, suggesting a close relationship to malignancy [12]. Evidence also suggested a process regulating CK6 through activator protein-1 binding, which may be regulated by c-fos and c-jun [13].

Type I also have a role in regulating cell growth. CK17 presence in the nucleus was shown to allow a complex to be formed by interaction with an integral membrane protein, LAP2β. This was thought to affect gene expression and cell proliferation [14]. CK18 was modified by phosphorylation at Ser 33 and Ser 52 sites, enabling it to interact with pathways regulated by parkin, a tumor suppressor [15]. Phosphorylated CK18 and CK19 interacted with 14-3-3 proteins, which promoted the solubility of cytokeratins and their recruitment to membranes [16, 17]. Whereas these modifications may modulate some of the non-mechanical functions of the cytokeratins, it is not known whether they affect growth. One possible way in which they could affect it is by regulating the formation of a CK8-Akt complex. It has been proposed that Akt binds to CK8 in the CK8/CK18 protofilament. Failing this interaction, it is hypophosphoryated specifically at a residue essential for activation. However, studies in which both CK8/CK18 were knocked down showed that Akt phosphorylation and activation were enhanced [18].

Previous studies have not addressed the question of whether any changes were related to oncogenic transformation but independent of the expression patterns associated with the tumors' differentiated state. Some 85% of human tumors originate from epithelial cells. As cytokeratins comprise a large fraction of the cytoskeleton, they could have an important role in growth control. Nevertheless, the profiles of tumors remained roughly similar to those in the tissue of origin (see for review [19]). Even in the normal state, the epithelial differentiation could be perturbed by chemical or physical agents, initiating changes in cytokeratin expression. For example, in upper airway epithelium, vitamin A deficiency caused the normal pseudostratified epithelium to be replaced by a metaplastic squamous epithelium [20]. This was accompanied by the disappearance of certain cytokeratins

and a marked increase in expression of one or more others [21]. Both *in vivo* [22] and *in vitro* [23, 24], CK18 expression was reduced while expression of CK13, a marker for cornified squamous epithelium, was increased. Changes in type II cytokeratins were also found, especially enhanced expression of CK4, typical of stratified epithelial tissues (see for review [22]). Another change following toxin exposure was a reduction in CK15 expression in submucosal glands [25]. Upon removal of the pathological stimulus, the squamous metaplasia was reversed along with the cytokeratin profile (see for review [26]).

The cytokeratins of airway tumors were dramatically different from the composition of the normal epithelium. In parallel to the differentiation of the epithelial lining into a squamous epithelium, tumors with a squamous differentiation expressed cytokeratins typical of squamous metaplasia, namely CK4 and CK10. In contrast, adenocarcinomas, which are thought to arise from hyperplastic adenomatous lesions, expressed keratins typical of mucous cells, namely CK7, CK8, and CK18 [27]. CK13 was present in most tumors showing squamous differentiation, while CK4 was found with CKs 7, 18, and 19 in adenocarcinomas of the lung and adenosquamous tumors [28]. These studies did not screen for "keratinocyte-type" K5/K14 pair which typically composed the filaments attached to hemidesmosomes and desmosomes [1], but these cytokeratins were also found in non-small cell lung cancer [29]. CK6 and, in some cases variable levels of CK14 and CK15, were identified in squamous cell carcinomas. Altogether, keratins CK4-CK8, 10, 13, 17, 18, and 19 were found in squamous cell carcinomas, although the exact pattern depended on the differentiated state of each tumor [30].

It was clear from the above studies that cytokeratin profiles from airway epithelium depended on differentiation to such an extent that it was difficult to infer a relationship to growth control. As the defects that enable epithelial cells to invade the submucosa and metastasize are of great interest, it was desirable to reinvestigate the cytokeratins' relationship to growth potential after having compensated for the cells' differentiated state. The cytokeratin profiles of epithelia originating from the same tissue source could be compared in a well-characterized *in vitro* model system for squamous cell carcinoma. In the tissue culture setting, physical barriers to expansion were removed, and cells entered the logarithmic phase of growth within 48 h of being subcultured. Moreover, the nutritional composition of the environment could be simplified by growing the cell lines in identical media. Three highly tumorigenic lines and three lines with lesser tumorigenic potential were used [31], and the question of whether cytokeratin profiles were related to the altered growth potential of epithelial cells was revisited.

2. Materials and methods

2.1 Primary cells and cell lines

Normal, primary epithelial cultures were grown out of tracheal explants from specific-pathogen-free, inbred F344 rats. The cultures were grown in a Waymouth's medium enriched with amino acids, putrescine, sodium pyruvate, hydrocortisone, insulin, fetal bovine serum, penicillin, and streptomycin [32, 33]. Cell lines were also from the upper airway epithelium of F344 rats. Nonmalignant lines were derived after treatment with 7,12-dimethylbenz(a)anthracene- or 12-0-tetradecanoylphorbol-13-acetate. They were tested in immune-suppressed host animals. They were found to be nontumorigenic at early passages but became tumorigenic after prolonged growth *in vitro* [31, 34–36]. Malignant cell lines were generated by treating tracheal tissues with benzo[a]pyrene (B2-1 and BP3) or 3-

methylcholanthrene (MCA7). The malignancy of the resulting tumors was increased further by serial passage in animals [37].

2.2 Characterization of malignancy and differentiation

To classify the cell lines by their growth potential, we determined the number of cells required to induce tumors in 50% of the animals tested (T.D.50). Cultured cells were injected into the thighs of immune-deficient rats or athymic nude mice, as previously described [31]. The highly malignant cell lines were tested by titrating the dose down from 1000 cells and determining the frequency with which tumors appeared by 43 weeks. These lines all produced invasive, keratinizing squamous cell carcinomas. To check for metastases, 1×10^4 cells were injected into the thigh, and the leg with the primary tumor was amputated 6 weeks after the injection date. Animals were euthanized and necropsied 6 weeks after the amputation.

Tissue differentiation was studied by removing tumors at 7–13 weeks after injection and preparing them for histological examination. They were bisected, fixed in 10% buffered formalin, and embedded in paraffin. Sections were cut at 6 μm thickness, mounted on slides and stained with hematoxylin and eosin.

The tendency of cells to undergo terminal keratinization *in vitro* was evaluated by examining cells dislodged from the surface of confluent cultures. A stream of medium was directed across the surface of the culture and the suspended cells were recovered by centrifugation at l200 $\times g$. Smears prepared from the pellets were fixed in 95% ethanol and stained by the Papanicolaou procedure [38].

2.3 Extraction of cytoskeletal proteins

To prepare the cytokeratins for 2D-PAGE, cells were plated at a density of 7–12 $\times 10^5$ per 100 mm dish and allowed to become confluent. A cytoskeletal preparation rich in keratins was made by the extraction procedure of Franke and coworkers [39]. Samples for isoelectric focusing were made by rinsing the dishes twice with TNM buffer (140 mM NaCl, 5 mM $MgCl_2$, 10 mM Tris-HCl, pH 7.6) and then treating them with 1% Triton X-100 for 4 min. The detergent-extracted cells were then washed twice with TMN, harvested with a rubber policeman, and pelleted by centrifugation at l500 $\times g$ at 4°C. An additional extraction was performed in some preparations. The culture dishes were rinsed with high salt TNM buffer containing 1.5 M KCl and 0.5% Triton X-100 for 10 min, and then the preparation was completed as above. The pellets were resuspended in sample buffer (2% SDS, 10% glycerol, 5% β-mercaptoethanol in 25 mM Tris-HCl, pH 8.3) and boiled until solubilized. Each sample was dialysed against 0.l mM phenylmethylsulfonylfluoride at 4°C. The dialysate was lyophilized and resolubilized in lysis buffer (9.S M urea, 2% Nonidet P-40, and 5% β-mercaptoethanol).

2.4 2D-PAGE and quantification of Coomassie blue staining intensity

Separation of proteins by their isoelectric point was performed by the method of O'Farrell [40]. Samples containing 300 μg of protein were run for 18–20 h in a gradient made up of LKB Ampholine pH 3.5–10. The pH profile in the first dimension was determined by measuring the pH in small sections of gels processed in parallel with those containing protein samples. After separation in the first dimension, each sample was electrophoresed into a 4% polyacrylamide stacking gel and 10% polyacrylamide resolving gel in a final concentration of 0.1% sodium dodecyl sulfate (SDS). For each cell line, 6–10 gels were run. In addition, some 150 μg samples were run to confirm the identity of the major protein species. The gels were

fixed in 12% trichloroacetic acid and stained with Coomassie blue, as previously described [40]. A lane of markers was added for the electrophoretic separation, including phosphorylase B (92.5 kDa), bovine serum albumin (66.2), ovalbumin (45.0), carbonic anhydrase (31.0) and soybean trypsin inhibitor (20.1). To analyze the total mass of cytoskeletal protein, samples were prepared with high-salt extraction, which ensured greater contrast between proteins and the background. A representative digital image from each line was selected, and the integrated absorbance at each spot on the gel estimated by comparison to the markers. After background subtraction, the boundaries around the spots were drawn manually, and the mass of each protein estimated by converting absorbance into intensity values, as previously described [41]. Total mass varied from ~60 to ~200 μg per gel.

2.5 Liquid chromatography-mass spectrometry-mass-spectrometry

For analysis by LC-MS-MS, proteins were excised from the gels, destained, reduced, alkylated, and trypsin-digested by a standard in-gel method. The peptides from each sample were concentrated and desalted using C18 Zip-Tip and reconstituted in 0.1% formic acid. Peptide mixtures were loaded onto a peptide trap cartridge and eluted onto a reversed-phase PicoFrit column (New Objective, Woburn, MA) as described elsewhere [42]. The eluted peptides were ionized and sprayed into the mass spectrometer, using a Nanospray Flex Ion Source ES071 (Thermo) and analyzed using a Thermo Scientific Q-Exactive hybrid Quadrupole-Orbitrap Mass Spectrometer and a Thermo Dionex UltiMate 3000 RSLCnano System.

Raw data files were searched against the rat protein sequences database using Proteome Discoverer 1.4 software (Thermo, San Jose, CA) based on the SEQUEST algorithm. Carbamidomethylation (+57.021 Da) of cysteines was set as a fixed modification, and oxidation/+15.995 Da (M), deamidated/+0.984 Da (N, Q), acetyl/+42.011 Da (K), phospho/+79.966 Da (S, T, Y), and ubiquitin-K/+114.043 Da (K) were set as dynamic modifications. The minimum peptide length was specified as five amino acids, and precursor mass tolerance was set to 15 ppm. The peptides' sequences and counts of peptide spectrum matches (PSM) were assembled into a Proteome Discoverer Report [42]. The effect of posttranslational modifications (PTMs) on the pI and MW of each protein were modeled using the Prot pi online bioinformatics tool [43].

2.6 Frequency and area analysis on gel spots and bands

For frequency analysis, spots on each gel were traced, converted to a binary image, and their areas were analyzed using the Particle Analysis module of ImageJ [44]. Under the assumption that each gel spot was a thin, continuous protein layer, the area was used to represent fractional volumes of each protein on the gel.

3. Results

3.1 Growth and differentiation of nonmalignant and malignant lines

Lines from the respiratory airway epithelium were divided into two groups on the basis of their abnormal growth potential as defined by their T.D.50 values. Tumor production required a 1000-fold greater number of nonmalignant cells than malignant cells (**Tables 1** and **2**). Moreover, none of the nonmalignant lines showed metastasis. Upon histological examination, all of the tumors had characteristics of invasive squamous cell carcinomas. The entire range of variation was represented

Tumorigenicity tests on cell lines of low malignant potential			
Cell line (passage)	Number of animals tested	Number with tumors	
		5×10^5	2×10^6
4C9 (17)	3	0/2	0/1
4C9 (38)	4	2/2	1/2
165S (16)	4	0/2	0/2
165S (32)	4	0/2	1/2
2C1 (13)	3	0/1	0/2
2C1 (23)	3	0/1	0/2

Table 1.
Cells of low malignancy tested in athymic nude mice.

Tumorigenicity tests on cell lines of high malignant potential				
Cell line	Animals tested	Number with tumors		
		1×10^2	3×10^2	1×10^3
B2-1 (37)	25	5/10	8/10	5/5
BP3-0 (1)	15	5/5	5/5	5/5
MCA7 (21)	30	9/10	10/10	10/10

Table 2.
Cells of high malignancy tested in immune-suppressed, isogenic F44 rats.

by the B2-l and BP3 lines, with MCA7 tumors showing intermediate histology between these two extremes. The keratinized cells of B2-1 tumors were squamous in shape but rarely if ever became enucleated. Even terminally differentiated cells showed small, pyknotic nuclei (**Figure 1a**). Internal portions of the B2-1 and MCA7 tumors became necrotic and also showed areas of infiltration by lymphatic cells. In BP3 tumors, multiple layers of enucleated squames were readily formed (**Figure 1b**). All three lines metastasized to the lymph nodes, and B2-1 also metastasized to the lung in 60% of the animals. The morphology of the metastases resembled that of the primary tumors (**Figure 1c**).

After injection with the specified number of cells, animals were maintained for 24–43 weeks. MCA7, the most immunogenic of the highly malignant cell lines, was tested similarly and formed tumors in 2 of 2 mice after injection of 1×10^3 cells. Modified from [31].

After injection with the specified number of cells, animals were maintained for up to 22 weeks. 165S (T15) was tested in 5 irradiated host animals at a dose of 1×10^3 cells and formed a tumor in one animal. The other nonmalignant lines were tested under similar conditions but failed to produce tumors. Modified from [31].

Normal and tumorigenic cells *in vitro* showed similar tendencies to form stratified squamous epithelia at high-density. The degree of squamous differentiation in confluent cultures could be assessed by imaging cells exfoliated from the cultures. In normal, primary cultures, the exfoliated cells were squamous in shape but did not become enucleated. The exfoliated cells from the lines differed in shape, but exfoliated cells from both primary cultures and cell lines commonly had pycnotic nuclei (**Figure 1D–G**).

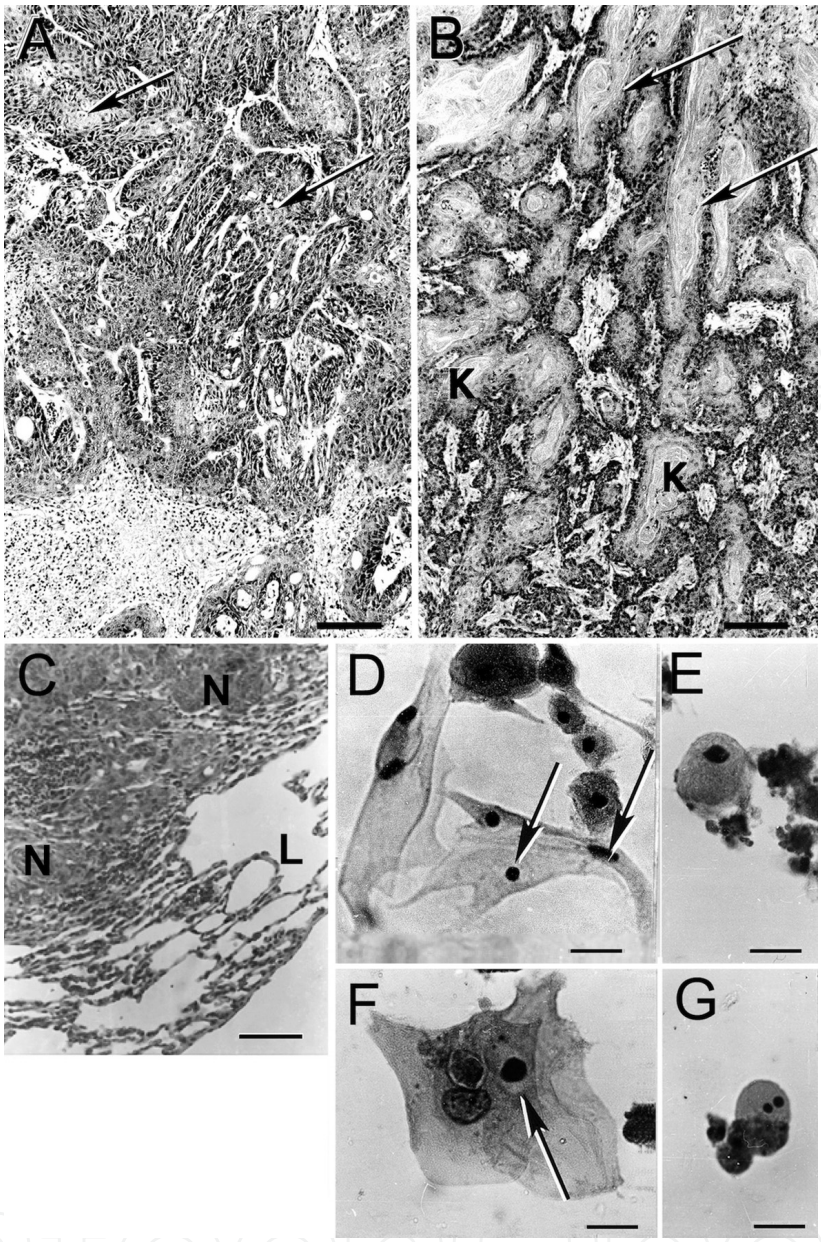

Figure 1.
Morphology of tumorigenic cells in vivo *and* in vitro*. (A) B2-1 tumor. The squamous cells in the outermost epithelial layer exhibit pycnotic nuclei (arrows). Invasion into the surrounding tissue containing blood vessels (bottom) is obvious. (B) BP3 tumor. Squamous cells of the differentiated epithelial layers show enucleated cells (arrows) resembling keratin "pearls" (K). Cells are invading into the mesenchyme at the bottom. (C) Border of a B2-1 metastasis to the lung. Nests of tumor cells (N) form at the boundary with the compressed lung tissue (L). (D–G) Exfoliated cells. (D) Squames from normal cell cultures with pycnotic nuclei (arrows), (E) BP3 with pyknotic nuclei, (F) 165S cells with pyknotic nuclei (arrow), (G) 4C9 cell. Bars, (A) and (B) 500 μm, (C) 200 μm, (D–G) 20 μm.*

3.2 Cytokeratins of normal epithelial cultures

Previous studies provided information about the keratin proteins of different cell types in the respiratory tract [1, 25, 28, 30, 45–53]. Methods for generating primary cultures were also well-known, and such cultures maintained the ability to repopulate normal epithelia after several weeks of growth *in vitro* [54]. Thus, the cytokeratins of the upper airways are summarized in **Tables 3** and **4**, and their presence or absence determined for cell lines differing in growth potential.

MW kDa, pI*	MW (rat)	pI (rat)	PTM (UniProt)		From LC-MS-MS	
			MW	pI	MW	pI
CK14†,‡			meth R, 1 phos		3 phos, 2 Ac	
50, 5.3	52.68	5.09	53.76	5.04	53.01	4.88
CK15†,‡,¶			7 phos			
50, 4.9	48.87	4.81	49.43	4.60		
CK19‡,§,¶,‖			9 phos, 5 meth R		2 Ac	
40–44 4.6–5.2	44.64	5.23	45.51	4.56	44.72	5.10
CK16‡						
46, 5.1	51.61	5.12				
CK17‡,§			2 phos		3 phos, 8 Ac	
48, 5.1	48.12	4.97	48.28	4.89	48.62	4.64
CK10			6 phos			
56.5, 5.3	56.50	5.11	56.90	4.90		
CK18†,§,¶			4 phos			
45, 5.1–5.7	47.76	5.19	48.08	4.99		
CK42	50.21	5.10				
β-Actin			Met oxidation		4 Ac	
41.7 5.2–5.3	41.74	5.32	41.77	5.32	41.91	5.03

**The MW (kDa) and pI on the left column are for human keratins [1]. Proteins of the same family are identified by colored typeface [55]. The effect of PTMs is modeled as described in Section 2. Abbreviations used are phos, phosphorylation; meth, methyl; Ac, acetylation.*
†Submucosal glands.
‡Basal cells.
§Clara cells.
¶Ciliated cells.
‖Cuboidal bronchiolar cells.

Table 3.
Type I proteins and β-actin between 4.6 and 5.3 pI compared to the human map.

Due to the fact that cytokeratins are highly conserved throughout evolution, it was possible to gather preliminary data by overlaying a map of the cytokeratins [1] on the proteins separated by 2D-PAGE. As shown in **Table 3**, the posttranslational modifications of CK14 and CK15 had minor effects on their position in 2D-PAGE, so they were used to center the map (**Figure 2a**). The spot representing CK17 (241 PSM) was confirmed by LC–MS–MS but also contained CK19 (99 PSM) and CK42 (97 PSM). The levels of the latter two appeared high as estimated by PSM, but were much lower than CK17 when the MS1 area of unique sequence was analyzed. These proteins, CK19 (89 PSM), CK17 (56 PSM), and CK42 (34 PSM), also made up the band at 42–43 kDa. CK42 was not displayed on the map of human cytokeratins [1], because it is a rodent cytokeratin that was lost in primates [56].

The CK5/CK14 pair was characteristic of basal cells of the normal mouse respiratory tract [52]. However, CK5 often occurred in the absence of CK14 in the human airway epithelium [57], and the latter was considered a marker for metaplasia [58]. Because primary tracheal cultures were largely made up of basal cells [59], the presence of the CK5/CK14 pair was anticipated. The CK14 spot was prominent, and the 56-kDa band contained both CK5 (311 PSM) and CK6A (272

MW kDa, pI*	MW (rat)	pI (rat)	PTM UniProt (1) LC-MS-MS (2)		From LC-MS-MS	
			MW	pI	MW	pI
CK4						
59, 7.3	57.67	7.24				
CK5†			(1) 11 phos (2) Met oxidation		3 Ac	
56, 7.4	61.83	7.37	62.71	5.22	61.95	6.20
			61.91	7.37		
CK6A†			(2) Met oxidation		8 Ac	
56, 7.8	59.25	7.62	59.33	7.62	59.58	5.72
CK7†,‡,§			(1) 8 phos		2 Ac	
36.7–54, 4.6–6.0	50.71	5.70	51.35	5.29	50.79	5.51
CK8‡,§			(1) 22 phos (2) Ac		5 Met oxidation	
49.7–54, 5.4–6.1	54.02	5.85	55.78	4.65	54.10	5.85
			54.10	5.60		

**The MW and pI on the left column are for human keratins [1]. Proteins of the same family are identified by colored typeface [55]. Abbreviations used are phos, phosphorylation; Ac, acetylation.*
†Basal cells.
‡Clara cells.
§Ciliated cells.

Table 4.
Type II cytokeratins of upper airways corresponding to pIs 4.6–7.8 of human.

PSM), as shown in **Figure 2b**. The amount of CK13, a marker of cornified squamous differentiation, was negligible, but another squamous cell marker, CK10, was sometimes present (**Figure 2a**).

Cells of the glands and gland ducts were previously shown to express CK14, CK15, CK18, and CK19 [45], and CK18 was also found in columnar and mucous cells [27]. CK8/CK18/CK19 characterized all columnar cells in the upper airways *in vivo*, including gland cells [28] and Clara cells [53], but were absent from basal cells of the bronchi [28, 45]. Whereas CK18 was not found in primary rat tracheal cultures, CK19 was present (**Figure 2b**). The band of 42–46 kDa spots contained both CK19 and CK42 and included β-actin. Although the theoretical range of β-actin pIs did not extend further than 5.3 (**Table 3**), β-actin in this band extended up to pI 6.1. CK8, which was shown to form heterodimers with both CK18 and CK19, was also present in primary cells. In addition, small amounts of CK7 were present (**Figure 2b**).

3.3 Is the cytokeratin profile changed by sequential passage of a cell line?

As oncogenic transformation generally gives rise to genomic instability, it is possible that sequential passage of a line might alter the cytokeratin expression. Samples from the 4C9 line were collected in passages 12–14 and compared to samples collected at passages 33 and 34. Proteins in the MW range of 45 kDa extended into more basic pIs in 4C9 than in normal cells, but this pattern was unchanged with passage levels. Similarly, bands of very low pI (less than 3.9) at approximately 61 and 55 kDA, were unaltered (cf. **Figure 2a** and **Figure 3a**).

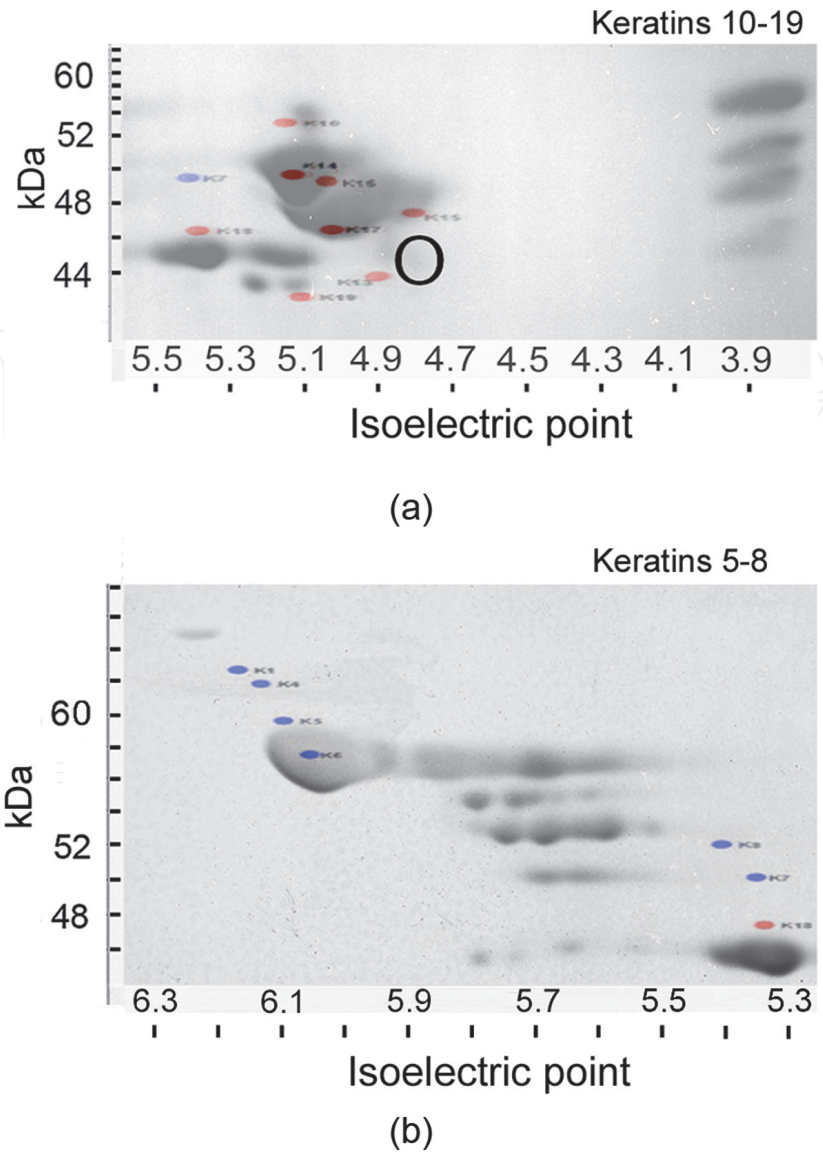

Figure 2.
Map of human cytokeratins [1] overlaid on a 2D-PAGE gel from normal tracheal epithelial cells. (a) Type I cytokeratins. There is a small spot at the site of CK10, and CK14 and CK17 are prominent. The proteins at 42–46 kDa are β-actin and CK19 mixed with degradation products from CK8 and CK5. At a highly acidic pI, the ubiquitinated CK14 and CK17 proteins are present (see ***Table 5****). (b) Type II cytokeratins. CK6A and CK5 are present at MW ~56 kDa, while low MW proteins, CK7 and CK8, migrate to lower pIs than other type II proteins. Proteins confirmed by LC-MS-MS analysis are underlined in* ***Tables 3*** *and* ***4****.*

Although a 4C9 sample from passage 33 showed a trace of CK13, this was also present in samples from the early passages. K13 was expressed in squamous metaplasia [22] and cultured tracheal cells [23]. The sporadic K13 spots observed in the current studies were consistent with the fact that, although the cells studied here showed signs of squamous differentiation, they were not cornified.

3.4 Differences in the actin and cytokeratins related to immortalization

The extension of the band containing actin and CK19 proteins into more basic pI ranges (cf. **Figures 2b** and **3a**) suggested that there may have been posttranslational modifications. Acetylation occurred on β-actin, as Lys61, Lys113, Lys213, Lys291, Lys315, Lys326, and Lys328 were found by LC-MS-MS. Modeling the addition of

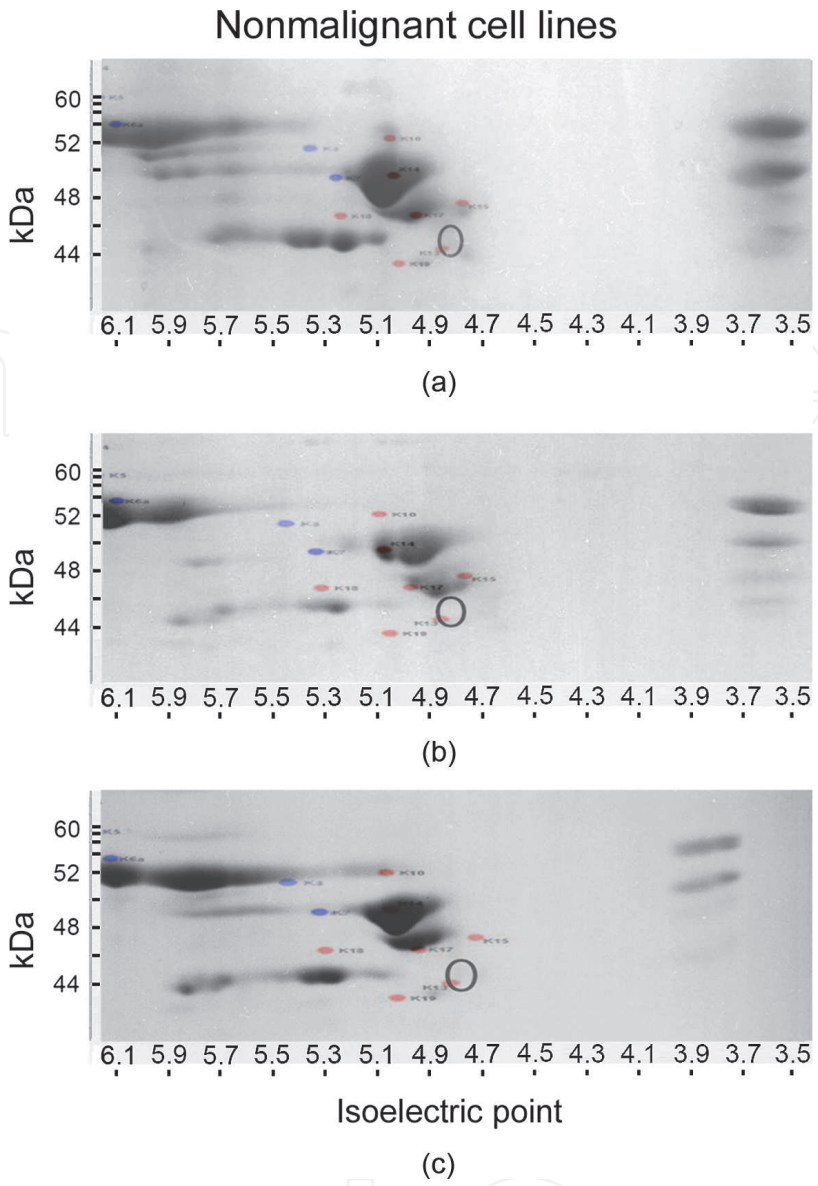

Figure 3.
*Cytokeratins from nonmalignant cell lines. The calculated MW is given in parentheses (see **Tables 3** and **4**). (a) 4C9. Type I cytokeratins, CK14 (53 kDa) and CK17 (48 kDa), are present along with actin and CK19 (below the marker for CK18) and type II CK5/CK6A (56 kDa) and CK8 (54 kDa). There is a faint spot in the region of CK13 (circled). Proteins present at high MW and pI of 3.5–3.9 are ubiquitinated CK14 and CK17. (b) 165S. The spot identified in (a) as CK14 (53 kDa) is resolved into two spots. CK7 (51 kDa) is present as a faint band below CK6A. (c) 2C1. The same cytokeratins are present as in (a) including a large amount of CK5/CK6A. As in (b), the β-actin/CK19 band extends beyond 5.8 pI.*

these residues together with Met sulfoxide modifications reported in the Uniprot database did not markedly change the predicted pI of β-actin, nor did any CK19 modifications found here shift the pI (**Table 3**). The 2C1 line, which had the lowest tumorigenic potential (**Table 1**), resembled 165S in the pIs of these 42–46 kDa proteins (cf. **Figure 3b** and **c**). The three lines showed slight differences in the cytokeratins of higher MW. In some 165S samples, the protein identified as CK14 was resolved into two spots (**Figure 3b**). The second was similar in MW but differed in pI, as would be expected for CK16. Likewise, in certain samples, the CK17 spot was resolved into two proteins. This is shown in a replicate 2D-PAGE experiment on the tumorigenic line (see Appendix, **Figure A1**). Trace amounts of

CK15 and CK16, found by LC-MS-MS analysis, were thought to reflect sporadic expression of these species. The spots sampled are shown in Appendix A (Portions of gel sampled for LC-MS-MS, **Figure A3**).

3.5 Cytokeratin profiles of malignant lines

The profile of samples from MCA7 and BP3 generally resembled normal cells. In particular, they had prominent bands containing CK8 (cf. **Figures 3b** and **4a-b**, and Appendix **Figure A2**). The mass represented in the type II cytokeratin, CK6A, declined in samples from all malignant lines, compared to primary and nonmalignant cells (cf. **Figures 3** and **4**). Unless the decrease in CK6A was

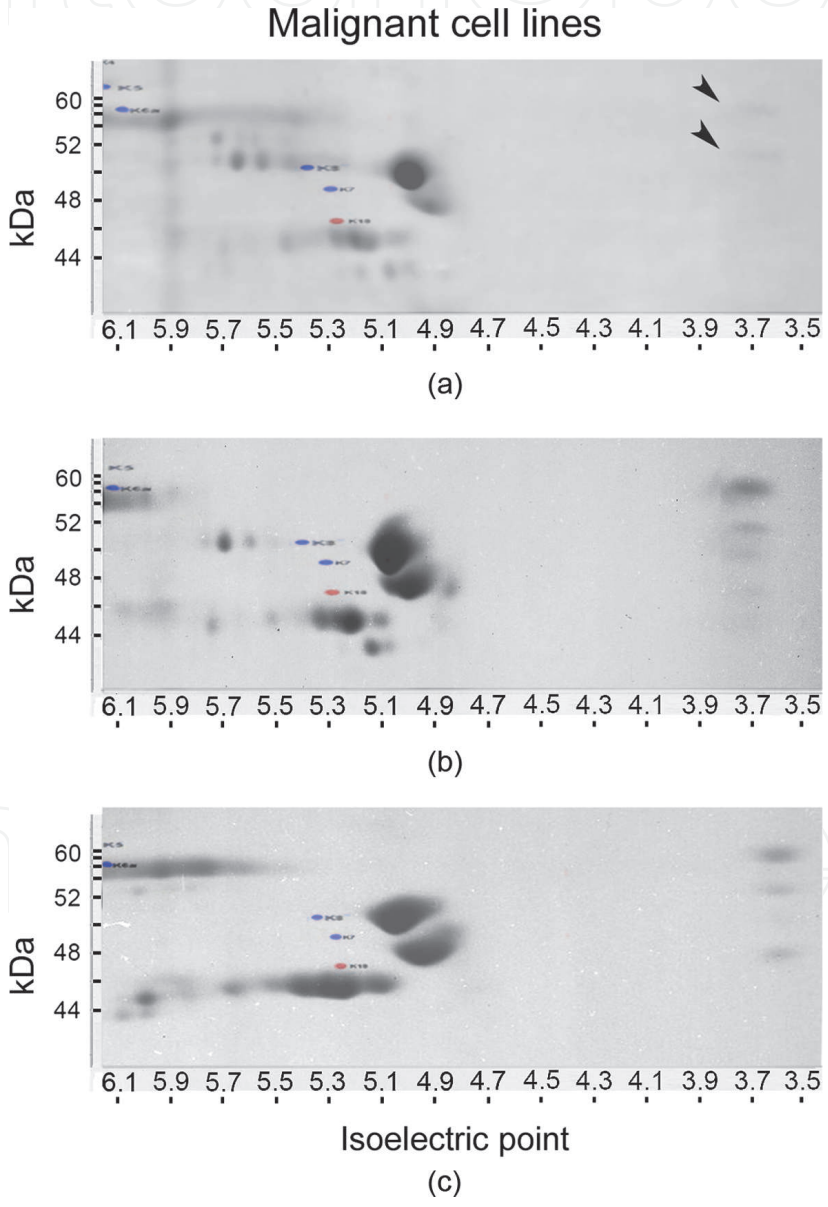

Figure 4.
*Cytokeratins from malignant cell lines. The calculated MW is given in parentheses (**Tables 3** and **4**). (a) MCA7. The type I CK14, CK17, and K19 were mapped, along with type II cytokeratins, CK5/CK6A (62 kDa/59 kDa), and CK8 (54 kDa). The actin/CK19 band occupies a similar range of pI as in normal cells. Faint bands are visible at pI 3.7 (arrowheads). (b) BP3. The profile resembles that in (a), except that the actin/CK19 range extends beyond 5.9. (c) B2–1. The profile resembles (a) and (b), but CK8 is absent and proteins of the actin/CK19 band are increased.*

accompanied by an increase in another type II protein or a reduction in type I proteins, it would mean an imbalance between acidic and basic cytokeratins. This implication was investigated by determining the frequency of observing each major cytokeratin in the nonmalignant and malignant lines. The results suggested that the decline in CK6A content occurred over the entire range of pIs (uppermost markers, **Figure 5a**). There were also changes in a lower MW range within the pI range, 5.8–6.0. The actin/CK19 band was slightly more apparent in malignant cell samples at the extreme end of the pI range (lowermost markers, **Figure 5a**). With respect to the type I cytokeratins, two spots were occasionally observed at the location of CK17 in BP3 samples (**Figure 5b**). CK15 may have been resolved from CK17 at this location, as mentioned above. Results of replicate experiments on the highly malignant lines are shown in Appendix **Figure A2**.

The implication that there was a reduced content of basic cytokeratins was further investigated by selecting a representative 2D-PAGE image for each line and measuring the intensities of all spots. The results suggested that CK6A was the predominant type II cytokeratin in all samples except those from B2-1 where it varied widely. Thus, the total levels of type II closely followed those of CK6A. In the B2-1 line, CK7/CK8, and CK19 were elevated (**Figure 5c**). Heterodimers formed

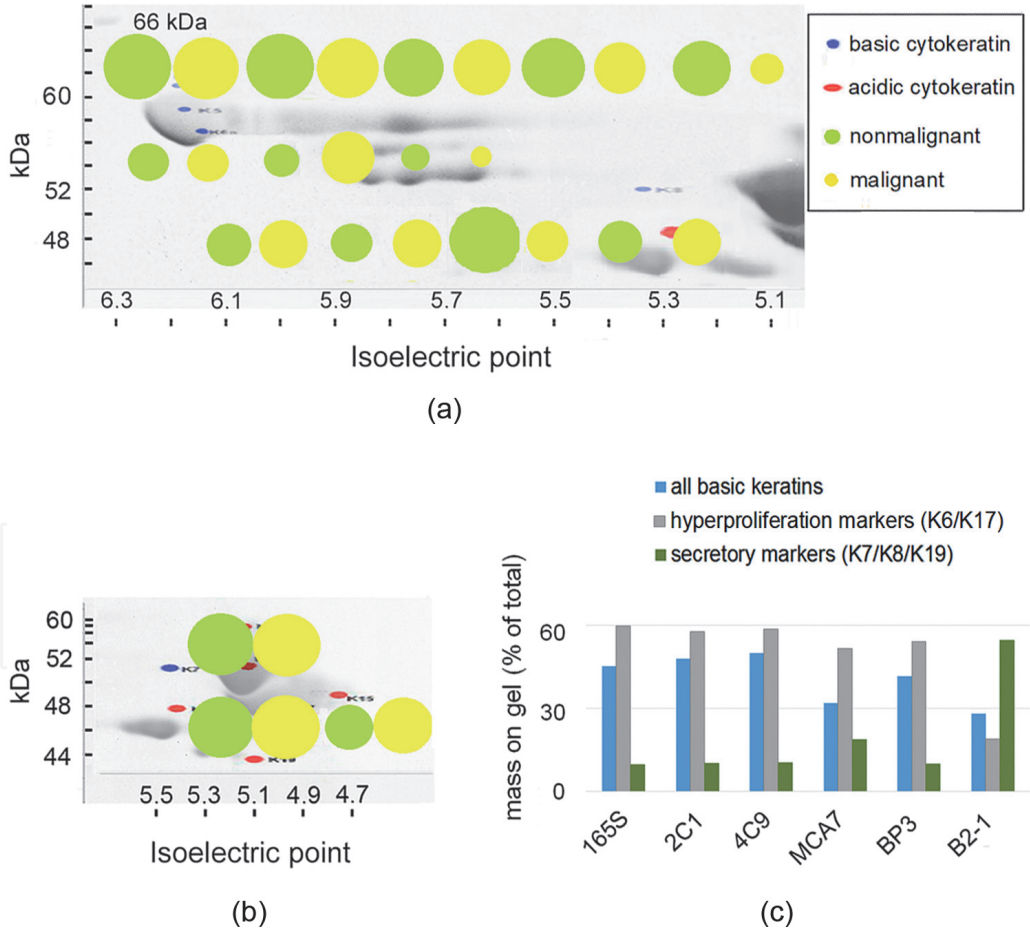

Figure 5.
Differences among the cytokeratins in selected samples from nonmalignant and malignant lines. (a, b) The frequency of observing a cytokeratin is represented by symbols for nonmalignant (green) and malignant (yellow). (a) Percentage of gels in which CK5/CK6A (uppermost), CK8 (middle), and the actin/CK19 band (lowermost) were present. (b) Percentage of gels in which CK14 (upper) and CK17 (lower) were present. (c) Content of type II cytokeratins and markers for secretory and hyperproliferating cells. Total type II content is similar to CK6A content except for the B2-1 line, where there is less CK6A. The results are representative of 27 gels.

between CK7/CK8 and CK19 were considered a marker for columnar or secretory cells (**Tables 3** and **4**). Interestingly, CK18 and CK19 were identified in sero (mucous) glands [28] and also found, along with CK7 and CK8, in large cell neuroendocrine carcinomas *in vivo* [60]. This suggested that B2-1 arose from a differentiated mucous, neuroendocrine, or Clara cell. Nevertheless, the total mass of type I cytokeratins also exceeded type II in the MCA7 line, which was apparently not derived from a differentiated cell type. Thus, the shortfall in type II content was not restricted to the B2-1 line.

3.6 Is there a general difference between nonmalignant and malignant?

While the results of **Figure 5** suggested a decrease of CK6A, a larger mass of protein in the 42–46 kDa band would automatically have reduced the amount of CK6A apparent at certain pI intervals. This band made up 25% of the mass in 2D-PAGE preparations from malignant MCA7 cells. The mass of protein in high MW/low pI bands was also variable (cf. **Figures 2** and **3**). For images in which most spots were present, a quantitative analysis was performed. To this end, the integrated intensities of proteins in the gels were computed in ImageJ. The results showed that these ubiquitinated protein bands were present in all cell lines and made up 9–18% of the total. The comparison also made it clear that lower CK5/CK6A content in the B2-1 line (**Figure 5c**) was accompanied by greater CK8 content (**Figure 6a**).

It is widely thought that cells maintain a stoichiometry of 1:1 type I to type II, and if any imbalance occurs, that they are able to restore the balance (see for review [9, 61]). If the entire type II keratin gene cluster was eliminated, the CK14 expression level was also reduced [62], (see for review [10]), suggesting a dependency of type I on type II expression. As the laddered arrangement of high MW bands at low pIs (<3.9) suggested addition of 8.6 kDa subunits from ubiquitin, LC-MS-MS was performed on tryptic digests to determine whether these proteins showed SUMOylation or ubiquitination. The main constituents were CK14 (317 PSM), CK17 (179 PSM), CK42 (91 PSM), CK19 (76 PSM), CK12/13 (58 PSM), and CK15 (41 PSM). Some type II proteins, CK6a (67 PSM) and CK5 (47 PSM), were also found. SUMO1-3 were not found, but sites of ubiquitin addition on CK14 and CK17 were identified (**Table 5**). For CK14 Lys153 and CK17 Lys374, the same residue was alternatively acetylated or ubiquitinated. Most of the peptide represented was in one of these two forms, suggesting near-universal modification at those sites. One of the ubiquitinated sites in CK17 (K172) was homologous to that of CK19 (**Table 6**). Thus, although the bands at very low pI contained some basic cytokeratins, the shortfall of type II content could not be explained by selective ubiquitination, as these bands were mainly composed of type I proteins (**Table 5**).

The reason for the extremely low pI of these proteins was unclear. While both CK14 and CK17 are acetylated, modeling the effect of this PTM only slightly changed the estimated pI (**Table 3**). Modeling the addition of both acetyl groups and ubiquitin B onto CK17 gave a pI of ~5.1 and MW of ~74 kDa. The acidic pIs may have been due to PTMs not detected, or the proteins' configurations may have changed, causing basic charges to be sequestered in regions of the protein that were relatively resistant to unfolding.

In skin *in vivo*, ubiquitination of CK14 levels occurred in the basal cells, and so the above data were consistent with the known mechanism whereby Kelch protein, Cul3 substrate adaptor, recruited CK14 for ubiquitination [63]. As ubiquitinated cytokeratins were more soluble in Triton X-100 [64], the fractionation method of the current experiments could have resulted in artifactual loss of ubiquitinated proteins. As mentioned above for mass determinations, this could have accounted for a shortfall in type I, but not type II cytokeratins. Another possible source of

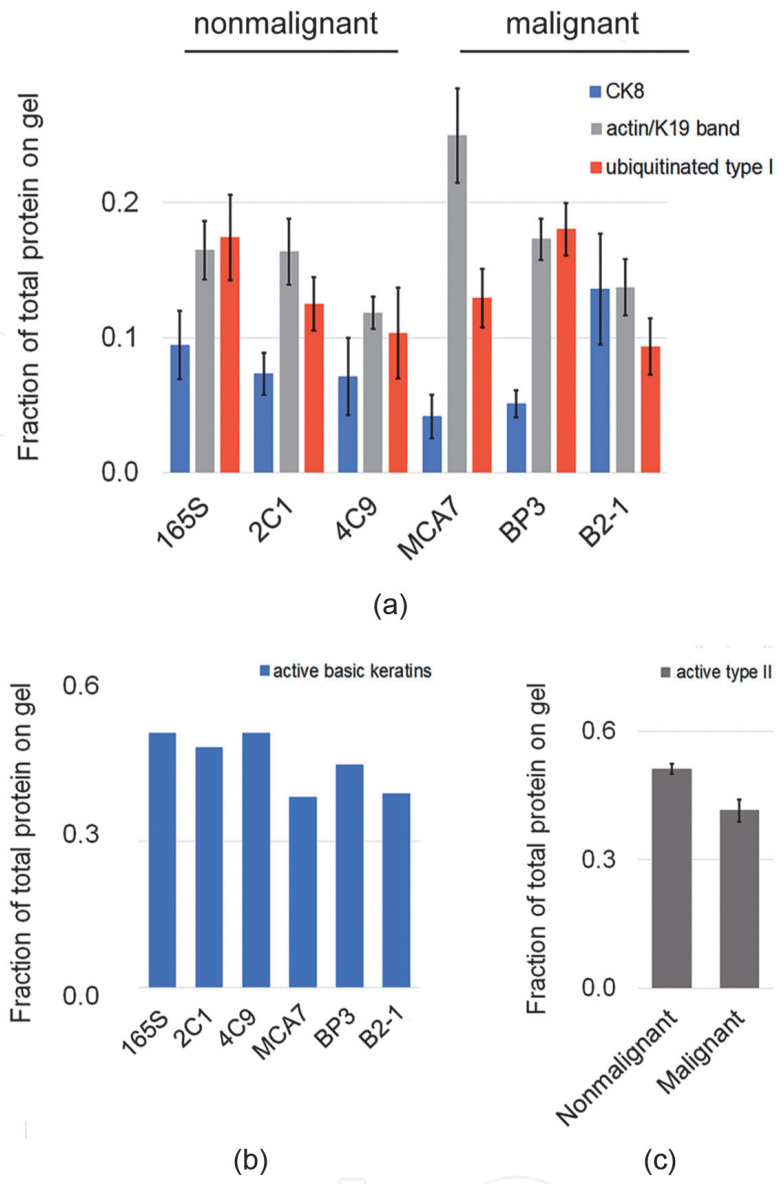

Figure 6.
Areas of spots identified on 2D-PAGE gels. The areas occupied were measured and represented as a fraction of the total area occupied by proteins on the gel. (a) Fraction occupied by CK8, bands of high MW and low pI, and proteins in the 42–46 kDa band. (b) Fraction of type II cytokeratins as a fraction of the total active cytokeratin, which was defined as the total area minus the area of the ubiquitinated cytokeratins. (c) Average integrated intensity of type II cytokeratins of nonmalignant versus malignant lines. Bars, ± standard error of the mean for 4–9 samples from each line.

artifact was phosphorylation, which again increased solubility and caused protein to be lost following dissolution of the filaments [4]. Although phosphosites were found in the current studies, they occurred in type I and type II alike (**Table 6**). As acetylation had a similar effect on solubility (see for review [10]), it is possible that the higher acetylation of CK6A accounted for some shortfall of the type II proteins.

Another source of artifact could be the variable mass of actin in the actin/CK19 band. Having been counted in the area of the acidic cytokeratins, the mass of actin could cause an artificial elevation in the mass counted as type I. MCA7 and 4C9 samples were at the opposite extremes of high and low 42–46 kDa content (**Figure 6a**). Despite being between these extreme values, BP3 cells still had less type II, suggesting that the actin band could not explain the effect overall. By assuming that the proteins at high MW and pI <3.9 were unavailable for filament

ID	Name	PTM	Peptide	With PTM (%)
Q6IFV1	CK14	Acetyl-K139	LATYLDKVR	54.5
		Acetyl-K153	ALEEANSDLEVKIR	83.6
		Ubi-K139	LATYLDKVR	4.0
		Ubi-K153	ALEEANSDLEVKIR	16.4
Q6IFU8	CK17	Acetyl-K172	TKFETEQALR	23.7
		Acetyl-K374	LLDVKTR	93.0
		Acetyl-K172	TKEFETEQALR	0.7%
		Ubi-K374	ILLDVKTR	2.5

[*]Ubiquitinated and acetylated sites of cytokeratins of high MW and low (<3.9) pI.

Table 5.
Ubiquitination in cytokeratin spots of high MW identified by LC-MS-MS.[*]

ID	CK	PTM	(First residue)	Site
Q6IFV1	14	Phos	(7) QFTSSSSMKGSCGIGGGSSR	T9
	14	Phos	(209) TKFETEQSLRINVESDINGLR	T213, S216
Q6IFU8	17	Phos	(7) QFTSSSSIKGSSGLGGGSSR	S13
	17	Ac	(130) DYSAYYQTIEDLKNK	K142
	17	Ac	(202) ADLEMQIENLKEELAYLKK	K212, 219, 220
	17	Ac	(408) TIVEEVQDGKVISSR	K420
Q6IFU7	42	Phos	(316) SVQNLEIELQSQLSM	S316
Q63279	19/17	Ac	(94) LASYLDKVR	K100
Q63279	19/17	Ac	(170) TKFETEQALR	K171
Q63279	19/17	Ubi	(170) TKFETEQALR	K171
Q63279	19	Ac	(144) ILGATIENSK	K153
	19	Ac	(257) SQYEAMAEKNRK	K265
Q6P6Q2	5	Phos	(30) TTFSSVSR	T30
	5	Phos	(45) VSLGGAYGAGGYGSR	S46
	5	Ac	(60) SLYNVGGSKR	K68
	5	Ubi	(60) SLYNVGGSKR	K68
	5	Ac	(274) DVDAAYMNKVELEA	K282
	5	Ac	(426) NKLTELEEALQK	K427, 437
	5	Ac	(262) TTAENEFVMLKK	K272
Q6IG12	7	Ac	(324) AKLESSIAEAEEQGE	K326
Q6IG12	7/8	Ac	(182) TAAENEFVLLKK	K192
Q6IG12	7/8	Ac	(388) KLLEGEESR	K388
Q6IG12	7/8	Ac	(91) TLNNKFASFIDK	K102
Q10758	8	Ac	(317) LQAEIDALKGQR	K325
Q4FZU2	6A	Ac	(150) TEEREQIKTLNNK	K157
	6A	Ac	(172) FLEQQNKVLDTK	K178
	6A	Ac	(240) SKYEDEINRR	K241

ID	CK	PTM	(First residue)	Site
	6A	Ac	(250) TAAENEFVTLKK	K260, 261
	6A	Ac	(328) AQYEEIAKR	K335
	6A	Phos, Glyc	(339) AEAESWYQTKYEELQITAGR	S342, O-GalNAc
	6A	Ac	(365) NTKQEISEINR	K367
	6A	Ac	(380) LRSEIDHVKK	K388
	6A	Ac	(389) KQIANLQAAIAEAEQ	K389
	6A	Ac	(414) GKLEGLEDALQK	K415
	6A	Ac	(433) LLKEYQDLMNVK	K435
	6A	Ac	(523) GISSGLSSSGGSSSTIK	K539
	6A	Glyc	(523) GISSGLSSSGGSSSTIK	S525

**PTMs are on unique peptides unless otherwise designated. Ac = acetyl, Phos = phosphate, Glyc = O-GalNAc, Ubi = ubiquitin.*

Table 6.
*PTMs identified by LC-MS-MS in the cytokeratins of airway epithelium.**

formation, it was possible to get an accurate estimate of the type I:type II ratio for each line. Type II proteins from nonmalignant cells made up 49–52% of the total (**Figure 6b** and **c**), suggesting a balance close to the hypothetical 1:1. In the malignant lines, basic cytokeratins constituted 39–46% of the total protein in 2D-PAGE gels. Despite its variability in malignant lines (**Figure 6c**), the lesser fractions suggested a shortfall of type II in the total cytokeratin fraction.

4. Discussion

Investigators' attempts to address the relationship between cytokeratins and growth control have been frustrated by the tremendous complexity of cytokeratin expression. In the current research, this was overcome by growing cells in media with the same composition and collecting them in the log phase of growth *in vitro*. This relieved the constraints of the *in vivo* environment. The cytokeratin profile became surprisingly similar to normal, primary cells, even for lines differing in growth potential *in vivo*. Despite the fact that the rat lines all formed squamous cell carcinomas upon testing in hosts, the cytokeratins typical of human airway squamous cell carcinomas *in vivo* [28] were much reduced. There was little representation of cornification markers, and CK4, the characteristic cytokeratin of stratified epithelia, was rare. In contrast, cytokeratins that were not prominent *in vivo*, e.g. CK6A and CK17, were present at high levels.

Thus, the conservatism of cytokeratin expression, which has made these proteins useful markers of a tumor's cell type of origin, was overcome by the *in vitro* conditions. Comparisons among the cultured lines suggested that B2-1 cells were derived from mucous cells or Clara cells, but otherwise there was a dearth of differentiation markers. For example, CK5/CK14 characterize the basal cells of compound epithelia, but the *in vitro* cultures showed CK5 levels that were far lower than CK14. The CK8/CK18 pair making up loose filaments, called "the simple-epithelial keratins", characterized the lumen linings of pseudostratified and complex epithelia (see for review [1]). This pair was found in most non-small cell lung cancer lines [65]. Whereas CK8 was present in most of the samples analyzed here, it was at lower levels than CK6A, except in the B2-1 line which apparently originated

from a columnar cell type. In the airway epithelium *in vivo*, CK6 and CK16 were upregulated during development of squamous metaplasia [22, 66], as was CK14 in proliferating airway cells [52]. CK6A, typically paired with CK16, was a marker of hyperproliferation and wound healing, but the current results suggested that CK17 substituted for CK16 in the airway epithelial cultures. The CK6A/CK17 pair characterized both normal cells, nonmalignant, and malignant cell lines, suggesting that it was a hyperproliferation marker and unrelated to malignancy.

One novel observation from these studies was that ~10% or more of the cytokeratin mass is ubiquitinated. These species do not seem to have been reported previously but may have been missed because they occupy very low pI regions after 2D-PAGE. Although these bands might represent disordered proteins that are being recycled, only ubiquitin-mediated targeting for degradation has been reported to date [61, 63, 64]. As very little type II cytokeratin content was found in the highly acidic, ubiquitinated bands, turnover mainly affected type I proteins. A previous proposal, based on knockout of the type II genes, held that acidic cytokeratins were degraded rapidly in the absence of basic cytokeratins [67]. This is supported by the current work. The type I and II cytokeratin content is normally equal, but the contents here were not equally weighted. If the ubiquitinated protein content had been included in the mass estimates, an even higher type I:type II ratio would have been represented. The shortfall, however, became noticeable in the lines of high malignancy.

Previous evidence suggested that high levels of CK8 can facilitate tumor progression (see for review [9]). Although CK8 levels were elevated in some samples of the metastasizing cell line, B2-1, this may reflect its derivation from a differentiated secretory cell rather than oncogenic transformation. On the other hand, the species of 42–46 kDa and high pI, especially CK19, are of interest. The samples from tumorigenic and malignant lines generally differed in the migration of CK19 and/or actin to higher pI. PTMs leading to a high pI in CK19 were previously associated with worse prognoses in adenocarcinoma [51]. While subcellular reorganization of cytokeratins is typical of cells with invasive or malignant traits [6, 31], it remains unclear whether this is due to signaling or merely mechanical properties. Some of the cytokeratins were implicated in signaling, but clear relationships to growth control were lacking. CK18 and CK19 bound 14-3-3 proteins (see Introduction) and Src kinase was inhibited by its association with CK6 [68]. If type I cytokeratin expression depended on the presence of type II, as suggested above, it is possible that greater turnover of acidic proteins occurred. This may account for the current finding of ubiquitylated proteins at low pI. Thus, further studies on the deficit in 1:1 ratio of basic to acidic cytokeratins may shed light on the mechanism of structural revision during tumor progression.

Acknowledgements

The author is grateful for the technical assistance of Yatish Shah, Ronald Manger, Greg Ridder, Marcella Williams, Carrie Greenway, Jon Hao, and Jessica Barnett.

A. Appendix

A.1 Portions of gel sampled for LC-MS-MS

The identity of the proteins on gels was determined by reference to a 4C9 sample. Six positions on the gel, shown on **Figure A3**, were excised for LC-MS-MS. The MS raw files can be found at pCloud.

https://u.pcloud.link/publink/show?code=kZuGtUXZjqkXZG6pCyJ-TO3VJHoKAWna7dM8gSU9gV

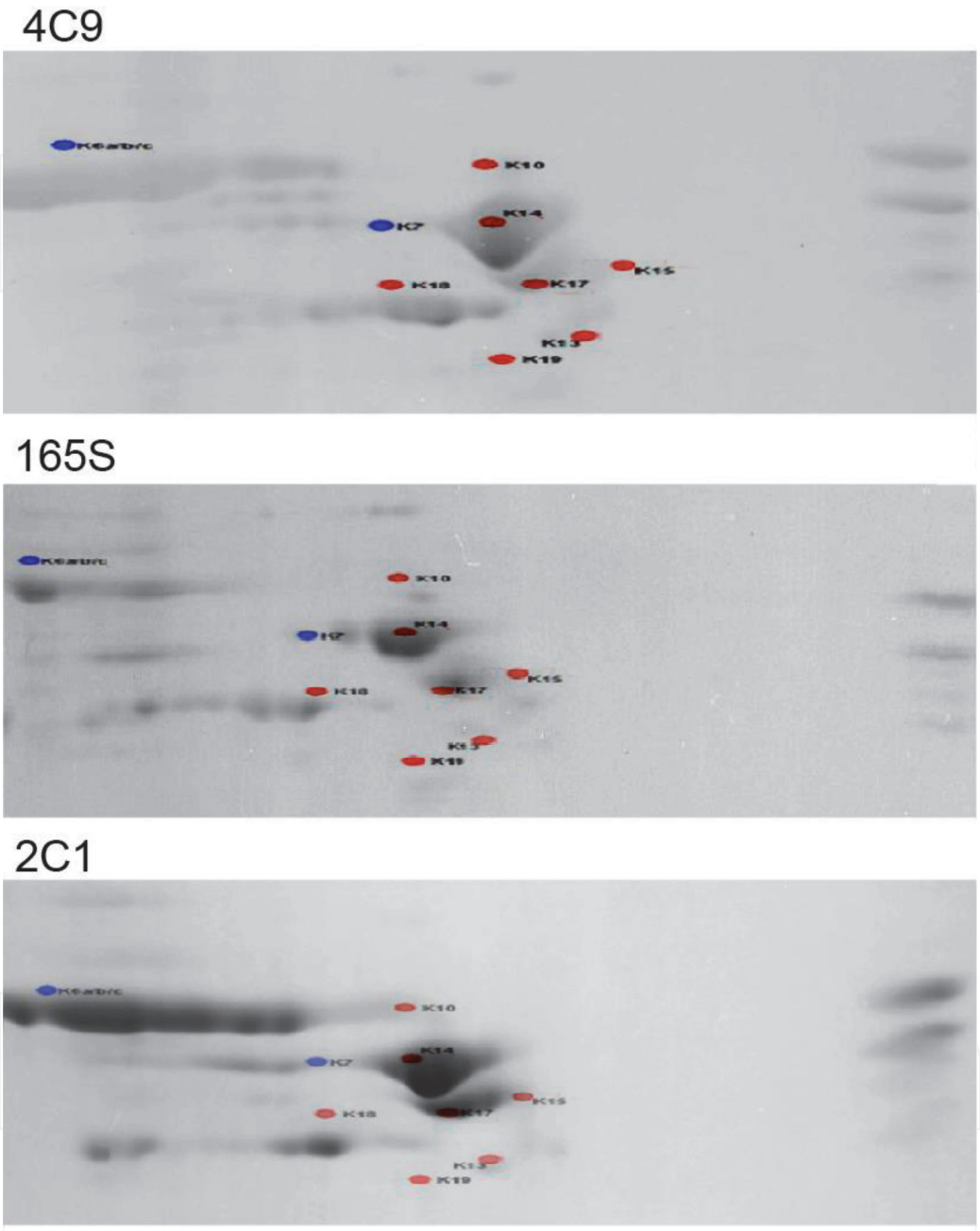

Figure A1.
Replicate experiments on cytokeratins from nonmalignant lines. In 4C9, CK14 (53 kDa) and CK17 (48 kDa) are present along with actin and CK19 (below the marker for human CK18) and type II CK5/CK6A (56 kDa) and CK8 (54 kDa). Bands are also present at high MW and low pI (3.5–3.9). In 165S, CK14 and CK17 are present, along with actin and CK19. Type II cytokeratins are represented by CK5/CK6A (56 kDa) and CK7 (51 kDa). In 2C1, the same cytokeratins are present as in 4C9.

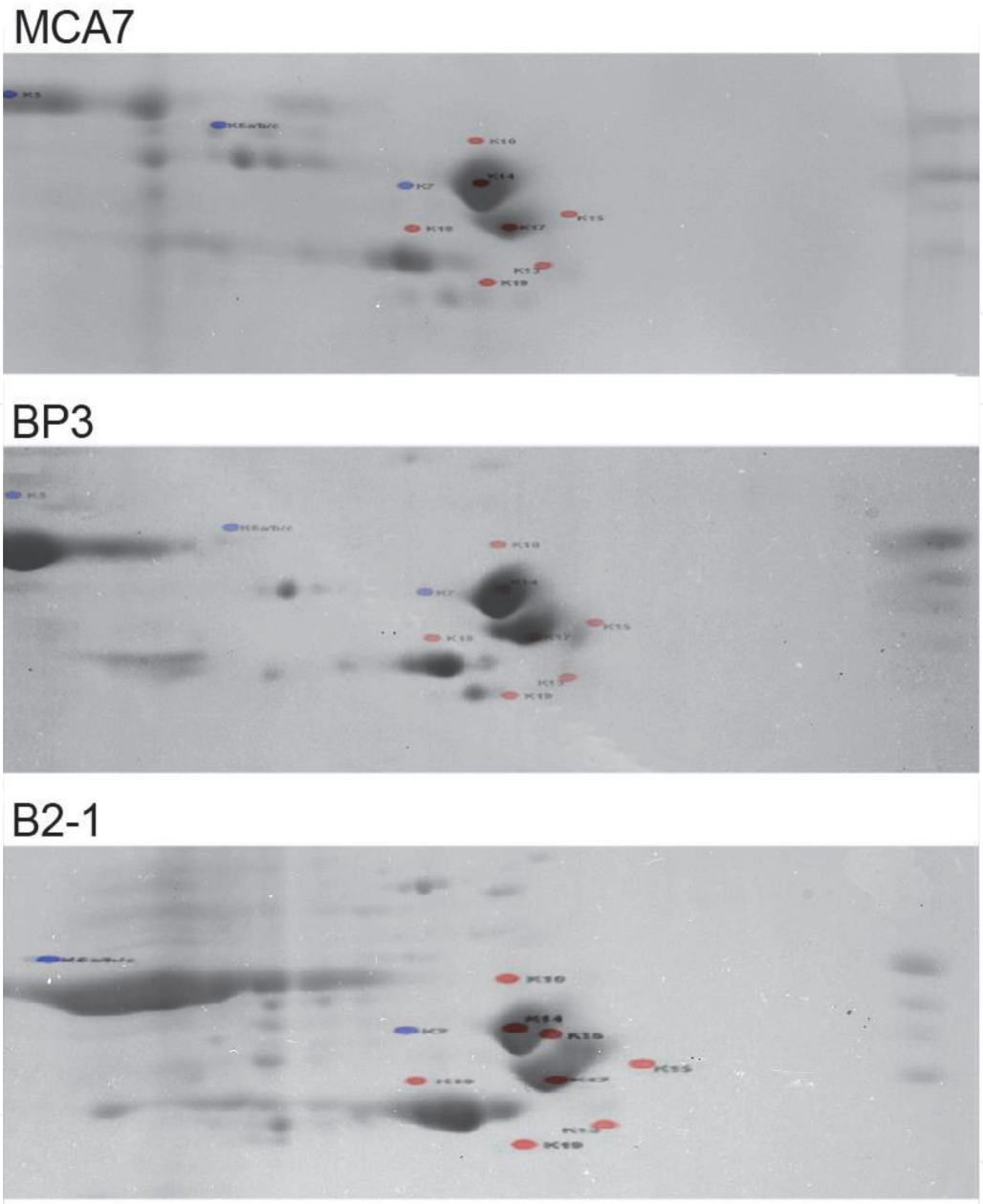

Figure A2.
Replicate experiments on cytokeratins from malignant lines. Type I cytokeratins, CK14 and CK17, were identified in all samples by reference to the map of human cytokeratins. Spots representing CK42 and CK19 are close to the CK18 marker. In MCA7, the type II cytokeratins found were CK5/CK6A (62 kDa/59 kDa), and CK8 (54 kDa). Faint bands are visible at low pI. In BP3, the profile is similar except that CK6A is the predominant type II cytokeratin. There is also a faint spot near the marker for CK15, as well as four bands at low pI. In B2-1, the CK8 band and proteins of the actin/CK42/CK19 band are prominent. Again, there are four discrete bands at low pI.

DOI: http://dx.doi.org/10.5772/intechopen.102592

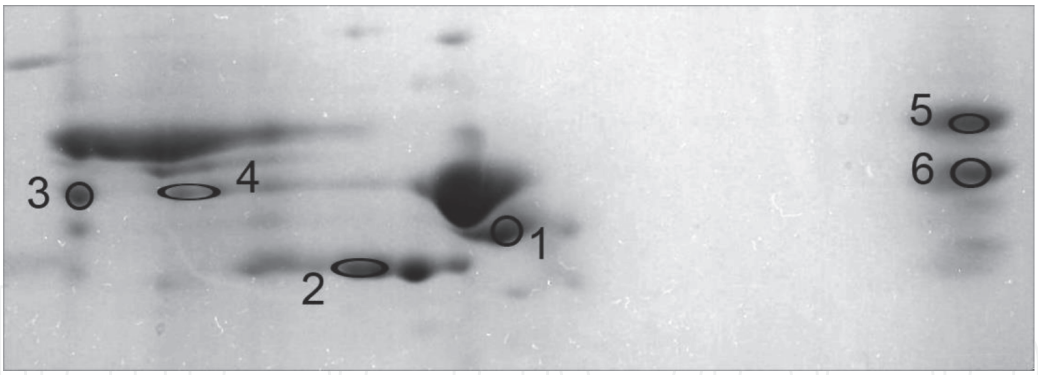

Figure A3.
Cytokeratins from 4C9 identified by LS-MS-MS.

Author details

Carol A. Heckman
Bowling Green State University, Bowling Green, Ohio, USA

*Address all correspondence to: heckman@bgsu.edu

References

[1] Moll R, Divo M, Langbein L. The human keratins: Biology and pathology. Histochemistry Cell Biology. 2008;**129**: 705-733

[2] Karantza V. Keratins in health and cancer: More than mere epithelial cell markers. Oncogene. 2011;**30**(2): 127-138

[3] Toivola DM, Zhou Q, English LS, Omary MB. Type II keratins are phosphorylated on a unique motif during stress and mitosis in tissues and cultured cells. Molecular Biology Cell. 2002;**13**(6):1857-1880

[4] Busch T, Armacki M, Eiseler T, Joodi G, Temme C, Jansen J, et al. Keratin 8 phosphorylation regulates keratin reorganization and migration of epithelial tumor cells. Journal Cell Science. 2012;**125**(Pt 9): 2148-2159

[5] Lane EB, Goodman SL, Trejdosiewicz LK. Disruption of the keratin filament network during epithelial cell division. EMBO Journal. 1982;**1**(11):1365-1372

[6] Seltmann K, Fritsch AW, Käsb JA, Magin TM. Keratins significantly contribute to cell stiffness and impact invasive behavior. PNAS USA. 2013; **110**(46):18507-18512

[7] Paladini RD, Takahashi K, Bravo NS, Coulombe PA. Onset of re-epithelialization after skin injury correlates with a reorganization of keratin filaments in wound edge keratinocytes: Defining a potential role for keratin 16. Journal Cell Biology. 1996;**132**(3):381-397

[8] Mazzalupo S, Wong P, Martin P, Coulombe PA. Role for keratins 6 and 17 during wound closure in embryonic mouse skin. Developmental Dynamics. 2003;**226**(2):356-365

[9] Dmello C, Srivastava SS, Tiwari R, Chaudhari PR, Sawant S, Vaidya MM. Multifaceted role of keratins in epithelial cell differentiation and transformation. Journal Biosciences. 2019;**44**(2):33

[10] Homberg M, Magin TM. Beyond expectations: Novel insights into epidermal keratin function and regulation. International Review Cell Molecular Biology. 2014;**311**(Chapter 6): 265-306

[11] Yang L, Zhang S, Wang G. Keratin 17 in disease pathogenesis: From cancer to dermatoses. Journal Pathology. 2018; **247**(2):158-165. DOI: 10.1002/path.5178

[12] Liu J, Liu L, Cao L, Wen Q. Keratin 17 promotes lung adenocarcinoma progression by enhancing cell proliferation and invasion. Medical Science Monitor. 2018;**24**:CLR4782-4790. DOI: 10.12659/MSM.909350

[13] Bernerd F, Magnaldo T, Freedberg IM, Blumenberg M. Expression of the carcinoma-associated keratin K6 and the role of AP-1 proto-oncoproteins. Gene Expression. 1993; **3**(2):187-199

[14] Jacob JT, Nair RR, Poll BG, Pineda CM, Hobbs RP, Matunis MJ, et al. Keratin 17 regulates nuclear morphology and chromatin organization. Journal Cell Science. 2020; **133**(20):jcs254094

[15] Song D-G, Kim YS, Jung BC, Rhee K-J, Pan C-H. Parkin induces upregulation of 40S ribosomal protein SA and posttranslational modification of cytokeratins 8 and 18 in human cervical cancer cells. Applied Biochemistry Biotechnology. 2013;**171**: 1630-1638

[16] Liao J, Omary MB. 14-3-3 proteins associate with phosphorylated simple

epithelial keratins during cell cycle progression and act as a solubility cofactor. Journal Cell Biology. 1996; **133**(2):345-357

[17] Mariani RA, Paranjpe S, Dobrowolski R, Weber GF. 14-3-3 targets keratin intermediate filaments to mechanically sensitive cell–cell contacts. Molecular Biology Cell. 2020;**31**(9): 930-943

[18] Fortier A-M, Asselin E, Cadrin M. Keratin 8 and 18 loss in epithelial cancer cells increases collective cell migration and cisplatin sensitivity through claudin1 up-regulation. Journal Biological Chemistry. 2013;**288**(16): 11555-11571

[19] Chu PG, Weiss LM. Keratin expression in human tissues and neoplasms. Histopathology. 2002;**40**(5): 403-439

[20] McDowell EM, Keenan KP, Huang M. Effects of vitamin A-deprivation on hamster tracheal epithelium: A quantitative morphologic study. Virchows Archiv B Cell Pathologie. 1984;**45**(2):197-219

[21] Huang FL, Roop DR, De Luca LM. Vitamin A deficiency and keratin biosynthesis in cultured hamster trachea. In Vitro Cellular Developmental Biology. 1986;**22**(4): 223-230

[22] Leube RE, Rustad TJ. Squamous cell metaplasia in the human lung: Molecular characteristics of epithelial stratification. Virchows Archiv B Cell pathology including molecular mathology. 1991;**61**(4):227-253

[23] Jetten AM, George MA, Smits HL, Vollberg TM. Keratin 13 expression is linked to squamous differentiation in rabbit tracheal epithelial cells and down-regulated by retinoic acid. Experimental Cell Research. 1989; **182**(2):622-634

[24] Kaartinen L, Nettesheim P, Adler KB, Randell SH. Rat tracheal epithelial cell differentiation in vitro. In Vitro Cellular Developmental Biology. 1993;**29A**(6):481-492

[25] Schlage WK, Bülles H, Friedrichs D, Kuhn M, Teredesai A, Terpstra PM. Cytokeratin expression patterns in the rat respiratory tract as markers of epithelial differentiation in inhalation toxicology. II. Changes in cytokeratin expression patterns following 8-day exposure to room-aged cigarette sidestream smoke. Toxicologic Pathology. 1998;**26**(3):344-360

[26] Jetten AM. Multistep process of squamous differentiation in tracheobronchial epithelial cells in vitro: Analogy with epidermal differentiation. Environmental Health Perspectives. 1989;**80**:149-160

[27] Wang GF, Lai MD, Yang RR, Chen PH, Su YY, Lv BJ, et al. Histological types and significance of bronchial epithelial dysplasia. Modern Pathology. 2006;**19**(3):429-437

[28] Broers JL, Ramaekers FC, Rot MK, Oostendorp T, Huysmans A, van Muijen GN, et al. Cytokeratins in different types of human lung cancer as monitored by chain-specific monoclonal antibodies. Cancer Research. 1988; **48**(11):3221-3229

[29] Chen Y, Cui T, Yang L, Mireskandari M, Knoesel T, Zhang Q, et al. The diagnostic value of cytokeratin 5/6, 14, 17, and 18 expression in human non-small cell lung cancer. Oncology. 2011;**80**(5–6):333-340

[30] Blobel GA, Moll R, Franke WW, Vogt-Moykopf I. Cytokeratins in normal lung and lung carcinomas I. adenocarcinomas, squamous cell carcinomas and cultured cell lines. Virchows Archiv B Cell pathology including molecular pathology. 1984; **45**(4):407-429

[31] Manger RL, Heckman CA. Structural anomalies of highly malignant respiratory tract epithelial cells. Cancer Research. 1982;**42**(11):4591-4599

[32] Heckman CA. Organ- and species-specificity of epithelial growth. In Vitro. 1983;**19**(1):31-40

[33] Marchok AC, Rhoton JC, Griesemer RA, Nettesheim P. Increased *in vitro* growth capacity of tracheal epithelium exposed *in vivo* to 7,12-dimethylbenz(a)anthracene. Cancer Research. 1977;**37**(6):1811-1821

[34] Marchok AC, Rhoton JC, Nettesheim P. *In vitro* development of oncogenicity in cell lines established from tracheal epithelium preexposed *in vivo* to 7,12-dimethylbenz(a) anthracene. Cancer Research. 1978; **38**(7):2030-2037

[35] Heckman CA, Olson AC. Morphological markers of oncogenic transformation in respiratory tract epithelial cells. Cancer Research. 1979; **39**(7):2390-2399

[36] Steele VE, Marchok AC, Nettesheim P. Establishment of epithelial cell lines following exposure of cultured tracheal epithelium to 12-O-tetradecanoyl-phorbol-13-acetate. Cancer Research. 1978;**38**(10):3563-3565

[37] Jamasbi RJ, Nettesheim P, Kennel SJ. Demonstration of cellular and humoral immunity to transplantable carcinomas derived from respiratory tracts of rats. Cancer Research. 1978;**38**(2):261-267

[38] Papanicolaou ON. Atlas of Exfoliative Cytology. Cambridge, MA: Harvard University Press; 1954. p. 202

[39] Franke WW, Mayer D, Schmid E, Denk H, Borenfreund E. Differences of expression of cytoskeletal proteins in cultured rat hepatocytes and hepatoma cells. Experimental Cell Research. 1981; **134**(2):345-365

[40] O'Farrell PH. High resolution two dimensional electrophoresis of proteins. Journal Biological Chemistry. 1975; **250**(10):4007-4021

[41] Ridder G, VonBargen E, Burgard D, Pickrum H, Williams E. Quantitative analysis and pattern recognition of two-dimensional electrophoresis gels. Clinical Chemistry. 1984;**30**(12 Pt 1):1919-1924

[42] Li R, Hao J, Fujiwara H, Xu M, Yang S, Dai S, et al. Analytical characterization of methyl-β-cyclodextrin for pharmacological activity to reduce lysosomal cholesterol accumulation in Niemann-Pick disease type C1 cells. ASSAY Drug Development Technologies. 2017;**15**(4):154-166

[43] Prot pi Protein Tool. Available from: https://www.protpi.ch/Calculator [Accessed: December 20, 2020]

[44] ImageJ. Available from: https://imagej.net/ImageJ1987 [Accessed: December 20, 2020]

[45] Schlage WK, Bülles H, Friedrichs D, Kuhn M, Teredesai A. Cytokeratin expression patterns in the rat respiratory tract as markers of epithelial differentiation in inhalation toxicology. I. Determination of normal cytokeratin expression patterns in nose, larynx, trachea, and lung. Toxicologic Pathology. 1998;**26**(3):324-343

[46] Bragulla HH, Homberger DG. Structure and functions of keratin proteins in simple, stratified, keratinized and cornified epithelia. Journal Anatomy. 2009;**214**(4):516-559

[47] Moll R, Franke WW, Schiller DL, Geiger B, Krepler R. The catalog of human cytokeratins: Patterns of expression in normal epithelia, tumors and cultured cells. Cell. 1982;**31**(1):1-24

[48] Moll R. Cytokeratine Als Differenzierungsmarker. Expressionsprofile von Epithelien Und

Epithelialen Tumoren [Cytokeratins as Markers of Differentiation. Expression Profiles in Epithelia and Epithelial Tumors]. New York: Gustav Fisher Verlag; 1993. pp. 1-197

[49] Foster MW, Gwinn WM, Kelly FL, Brass DM, Valente AM, Moseley MA, et al. Proteomic analysis of primary human airway epithelial cells exposed to the respiratory toxicant diacetyl. Journal Proteome Research. 2017;**16**(2):538-549

[50] Hackett NR, Shaykhiev R, Walters MS, Wang R, Zwick RK, Ferris B, et al. The human airway epithelial basal cell transcriptome. PLoS One. 2011;**6**(5):e18378

[51] Gharib TG, Chen G, Wang H, Huang C-C, Prescott MS, Shedden K, et al. Proteomic analysis of cytokeratin isoforms uncovers association with survival in lung adenocarcinoma. Neoplasia. 2002;**4**(5):440-448

[52] Cole BB, Smith RW, Jenkins KM, Graham BB, Reynolds PR, Reynolds SD. Tracheal basal cells: A facultative progenitor cell pool. American Journal Pathology. 2010;**177**(1):362-376

[53] Nakajima M, Kawanami O, Jin E, Ghazizadeh M, Honda M, Asano G, et al. Immunohistochemical and ultrastructural studies of basal cells, Clara cells and bronchiolar cuboidal cells in normal human airways. Pathology International. 1998;**48**(12):944-953

[54] Terzaghi M, Nettesheim P, Williams ML. Repopulation of denuded tracheal grafts with normal, preneoplastic, and neoplastic epithelial cell populations. Cancer Research. 1978;**38**:4546-4553

[55] Wang F, Zieman A, Coulombe PA. Skin keratins. Methods Enzymology, "Intermediate Filament Proteins". 2016; **568**:303-350

[56] Tong X, Coulombe PA. A novel mouse type I intermediate filament gene, keratin 17n (K17n), exhibits preferred expression in nail tissue. Journal Investigative Dermatology. 2004;**122**(4):965-970

[57] Ooi AT, Mah V, Nickerson DW, Gilbert JL, Ha VL, E. A, et al. Presence of a putative tumor-initiating progenitor cell population predicts poor prognosis in smokers with non-small cell lung cancer. Cancer Research. 2010;**70**(16): 6639-6648

[58] Smirnova NF, Schamberger AC, Nayakanti S, Hatz R, Behr J, Eickelberg O. Detection and quantification of epithelial progenitor cell populations in human healthy and IPF lungs. Respiratory Research. 2016;**17**:83

[59] Heckman CA, Marchok AC, Nettesheim P. Respiratory tract epithelium in primary culture: Concurrent growth and differentiation during establishment. Journal Cell Science. 1978;**32**:269-291

[60] Nagashio R, Sato Y, Matsumoto T, Kageyama T, Satoh Y, Ryuge S, et al. Significant high expression of cytokeratins 7, 8, 18, 19 in pulmonary large cell neuroendocrine carcinomas, compared to small cell lung carcinomas. Pathology International. 2010;**60**(2): 71-77

[61] Rogel MR, Jaitovich A, Ridge KM. The role of the ubiquitin proteasome pathway in keratin intermediate filament protein degradation. Proceedings American Thoracic Society. 2010;**7**(1):71-76

[62] Bär J, Kumar V, Roth W, Richter M, Leube RE, Magin TM. Skin fragility and impaired desmosomal adhesion in mice lacking all keratins. Journal Investigative Dermatology. 2014;**134**(4):1012-1022

[63] Lin A, Li S, Feng C, Yang S, Wang H, Ma D, et al. Stabilizing mutations of KLHL24 ubiquitin ligase cause loss of keratin 14 and human skin

fragility. Nature Genetics. 2016;**48**(12): 1508-1516

[64] Jaitovich A, Mehta S, Ciechanover A, Goldman RD, Ridge KM. Ubiquitin-proteasome-mediated degradation of keratin intermediate filaments in mechanically stimulated A549 cells. Journal Biological Chemistry. 2008;**283**(37):25348-25355

[65] Kanaji N, Bandoh S, Ishii T, Fujita J, Ishida T, Matsunaga T, et al. Cytokeratins negatively regulate the invasive potential of lung cancer cell lines. Oncology Reports. 2011;**26**(4): 763-768

[66] Stosiek P, Kasper M, Moll R. Changes in cytokeratin expression accompany squamous metaplasia of the human respiratory epithelium. Virchows Archiv A Pathological Anatomy. 1992;**421**(2):133-141

[67] Vijayaraj P, Kröger C, Reuter U, Windoffer R, Leube RE. Magin TM keratins regulate protein biosynthesis through localization of GLUT1 and −3 upstream of AMP kinase and raptor. Journal Cell Biology. 2009;**187**(2): 175-184

[68] Rotty JD, Coulombe PA. A wound-induced keratin inhibits Src activity during keratinocyte migration and tissue repair. Journal Cell Biology. 2012; **197**(3):381-389